

Silicon Angular Rate Sensor Using PZT Thin Film

Masaru Nagao, Kazuyuki Minami¹ and Masayoshi Esashi¹

Toyota Motor Corporation, 1 Toyota-cho, Toyota, Aichi 471-8571, Japan

¹Faculty of Engineering, Tohoku University
Aza-Aoba, Aramaki, Aoba-ku, Sendai 980-0845, Japan

(Received January 1, 1998; accepted August 18, 1998)

Keywords: silicon, gyroscope, angular rate sensor, PZT

A silicon resonant angular rate sensor using lead zirconate titanate ($\text{Pb}(\text{Zr}, \text{Ti})\text{O}_3$, or PZT) thin film for detecting sensor vibration was fabricated by silicon micromachining technology, and its basic properties were examined. PZT was deposited on a silicon wafer directly with a multitarget sputtering system. Since fabricated PZT thin films have poor piezoelectric characteristics, these films could not be used for driving the mass of the sensor. For this reason, the mass of the sensor was driven by an external piezoelectric actuator instead of PZT films. The test device could be successfully used as an angular rate sensor.

1. Introduction

Since lead zirconate titanate ($\text{Pb}(\text{Zr}, \text{Ti})\text{O}_3$, or PZT) has good ferroelectric properties, a great deal of effort has been focused on making PZT thin films for IC memory applications and pyroelectric infrared sensors. There is also a growing need to use PZT thin films in mechanical sensors and actuators using silicon micromachining technology because PZT has good piezoelectric properties.^(1,2)

Bulk PZT has been used for resonant angular rate sensor to drive the resonator and to detect sensor vibration, because PZT has high driving force and high sensitivity to stress (vibration). However, in the case of silicon resonant angular rate sensor, most of the sensors that have been reported to use electrostatic⁽³⁾ or electromagnetic⁽⁴⁾ force to drive the resonator and vibration is detected by capacitance changes.⁽³⁻⁵⁾

Address for correspondence

Masaru Nagao: Toyota Motor Corporation, Hirose Plant, 543 Kirigahora, Nishihirose-cho, Toyota, Aichi 470-0309, Japan

In this paper, we describe a silicon angular rate sensor that uses sputtered PZT thin film for detecting sensor vibration.

2. Sensor Structure and Principle

Figure 1 shows the structure of the fabricated sensor. This sensor consists of a frame, a glass mass (4.5 mm wide, 4.2 mm long) and two thin silicon beams that support the mass (3 mm wide, 1 mm long). On these silicon beams, PZT thin film and electrodes are formed to drive the sensor and detect sensor vibration. Each electrode has an area of about 1.2 mm². Figure 2 shows the working principle of the sensor. Silicon beams are bent by an AC voltage applied to drive electrodes resulting in the excitation of the vibration of the mass in the Z direction (excitation mode). When angular rate Ω is applied around the Y-axis, a Coriolis force in the X direction is produced. This Coriolis force causes the mass to oscillate around the Y-axis (detection mode). The angular rate can be determined by detecting this oscillation around the Y-axis. These two vibration modes (excitation mode and detection mode) are translated into electrical signals by PZT thin films on silicon beams.

Resonant frequencies of these two vibration modes (excitation mode and detection mode) are very important parameters for resonant angular rate sensors because they are strongly related to the sensitivity of resonant angular rate sensors. Mismatching of these two resonant frequencies results in low sensitivity of the sensor. From this point of view,

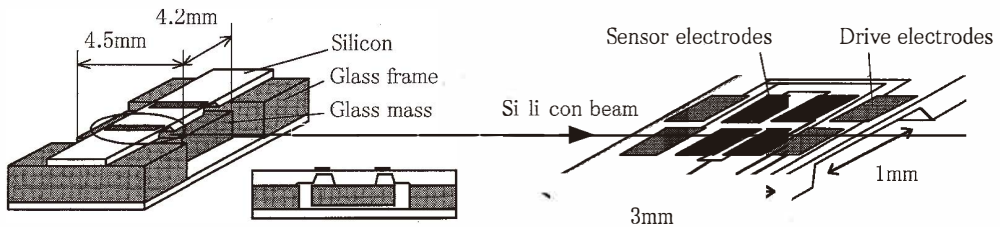


Fig. 1. Schematic views of the sensor structure.

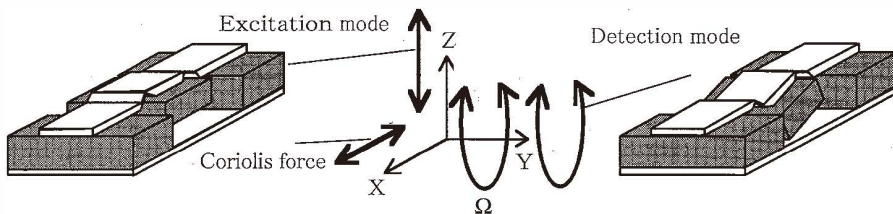


Fig. 2. Working principle of the sensor.

the structure shown in Fig. 1 is suited for an angular rate sensor because resonant frequencies of the two vibration modes can be determined from the size of the mass in the X direction. Figure 3 shows the result of the finite-element method (FEM) analysis of the relationship between resonant frequency and mass size in the X direction. On the other hand, mismatching of resonant frequencies is not caused by the variation of silicon beam thickness which strongly depends on process conditions. Figure 4 shows the result of the FEM analysis of the relationship between resonant frequency and silicon beam thickness. From these results, it is found that resonant frequencies can be determined from the mass size in the X direction.

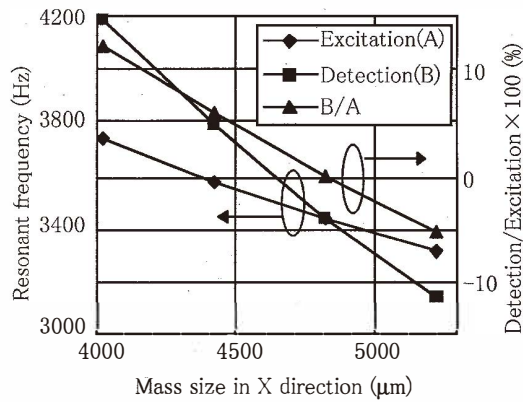


Fig. 3. FEM analysis of the relationship between resonant frequency and mass size in the X direction.

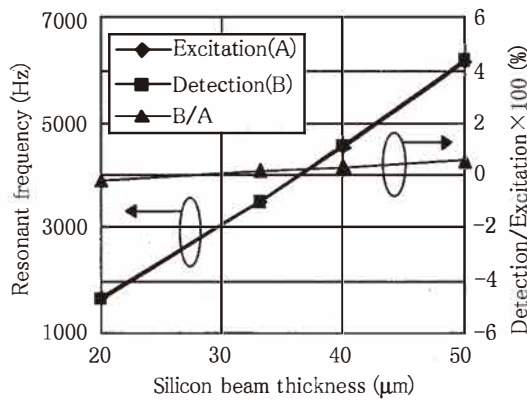


Fig. 4. FEM analysis of the relationship between resonant frequency and silicon beam thickness.

3. Fabrication

3.1 Fabrication of PZT thin film

Many methods for depositing PZT films have been proposed so far: the sol-gel method, chemical vapor deposition, laser ablation and sputtering. Among them, we chose the sputtering method because many previous works have been reported on this and we can easily obtain a fabrication system and source materials. However, it is reported that this method has a problem in that the film composition deviates from the sputtering target composition. The control of film composition is very important because the properties of PZT film drastically change with changes in composition. We used a multitarget rf-magnetron sputtering system to solve this problem. This system, shown in Fig. 5, has three targets, shutters, a rotating substrate holder and a lamp heater to control substrate temperature. In this experiment, a PZT target and a PbO target were used. The PbO target was employed to compensate Pb deficiency because, in most sputtering conditions, Pb content in the sputtered PZT film is less than that in the target. PZT and PbO are mixed in the deposited film by rotating the substrate holder shown in Fig. 5. Pb content was controlled by the deposition time ratio of PbO to PZT. The deposition time ratio was changed by the shutter in front of the PbO target. The ratio of Zr to Ti in the PZT target was 55:45 because bulk PZT of this composition shows good piezoelectric properties.

The sputtering conditions of PZT thin films were evaluated by measuring dielectric constants and remanent polarization. Figure 6 shows the sample structure. PZT (500 nm) and Pt/Cr for upper electrode were deposited on a Pt/Ti/SiO₂/Si substrate. Pt/Cr (50 nm/40 nm) and Pt/Ti (150 nm/50 nm) electrodes were deposited by electron beam evaporation.

3.2 Sensor process

Figure 7 illustrates the sensor fabrication process. Double-side polished silicon wafer (n-type, 400 μm thick) is used.

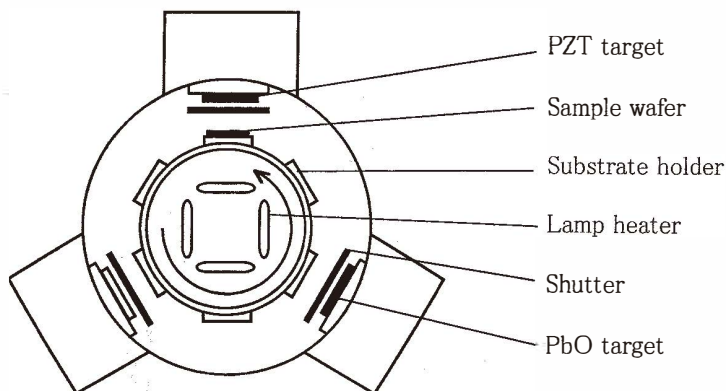


Fig. 5. Multitarget rf-magnetron sputtering system.

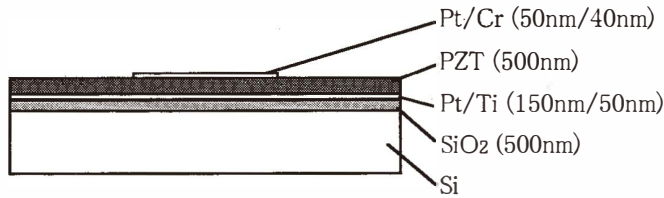


Fig. 6. Sample structure used for the evaluation of PZT thin films.

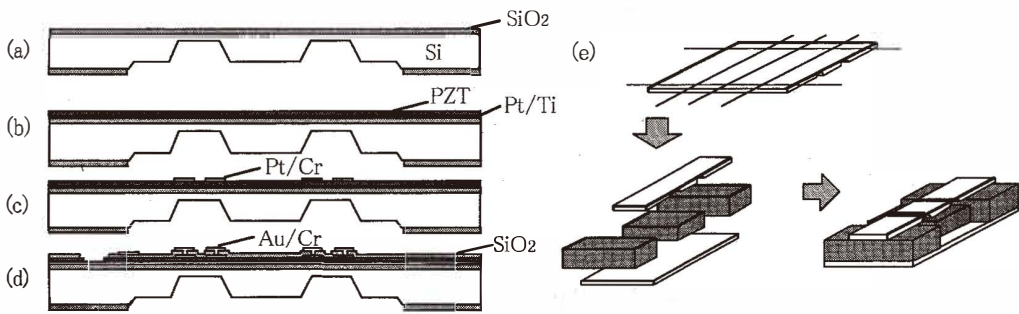


Fig. 7. Sensor fabrication process.

- a) After the silicon wafer is oxidized (500 nm thick), silicon is etched by TMAH with SiO₂ etching mask to make thin silicon beams (50 μm thick).
- b) Pt/Ti (150 nm/50 nm), which is used for the lower electrode, is deposited on the silicon by electron beam evaporation. PZT (500 nm) is deposited on Pt/Ti by sputtering.
- c) Pt/Cr (50 nm/40 nm) is deposited by electron beam evaporation. Pt/Cr is patterned by the lift-off method for the upper electrode.
- d) After the SiO₂ isolation layer (500 nm) is deposited and patterned, an Au/Cr (500 nm/50 nm) wiring layer is deposited and patterned. The PZT layer is etched out to expose the lower electrode.
- e) The wafer is diced, and the chip is bonded with the glass (mass and supports).

4. Results and Discussion

4.1 Properties of PZT thin film

Table 1 shows the sputtering conditions for PZT thin films. Since the substrate temperature is too low to form perovskite-phase PZT film that shows good piezoelectric properties, the as-grown sputtered PZT is an amorphous film. Thermal annealing is

Table 1
Sputtering conditions.

Substrate	Thickness	Pt/Ti/SiO ₂ (150 nm/50 nm/500 nm)
	Temperature	250°C
	Rotation speed	40 rpm
Sputtering environment	Ar : O ₂	5 : 1
	Pressure	5 mTorr
Target diameter		3 inch
RF power	PZT	100 W
	PbO	15 W

performed to transform the film from amorphous to perovskite phase. The annealing temperature and time are respectively 600°C and 30 min. Figure 8 shows the relationship between deposition time ratio and dielectric constant and remnant polarization. Remnant polarization was measured with a modified Sawyer-Tower circuit. A maximum remnant polarization of 13 $\mu\text{C}/\text{cm}^2$ and a maximum dielectric constant of 1000 were achieved at a deposition time ratio of 0.3 (PbO deposition time/PZT deposition time).

Piezoelectric properties were also evaluated by detecting sensor vibration. Figure 9 shows the evaluation circuit. Sensor vibration was applied using an external piezoelectric actuator, and an electric charge amplifier was used to sense electric charge from the PZT thin film. We estimated the piezoelectric constant from the vibration amplitude and the output signal. The estimated piezoelectric constant d_{31} of PZT thin film is about 1.44×10^{-12} C/N, which is about 1/100 of bulk PZT and is not sufficient to drive the sensor vibration. The measured sample also shows poor dielectric constant (300). We assume that these poor properties originate from the sensor fabrication process after PZT deposition because the sample after PZT film deposition showed dielectric constant of 1000.

4.2 Characteristics of the angular rate sensor

Since the fabricated PZT thin film has poor piezoelectric characteristics, the film cannot be used for driving the sensor. For this reason, the mass of the sensor was driven by an external piezoelectric actuator instead of the PZT film.

Resonance characteristics of the sensor were measured by the circuit shown in Fig. 9. The vibration signals of the excitation mode and the detection mode can be obtained by the sum or the difference of two signals from two silicon beams. Figure 10 shows the measured resonance characteristics of two vibration modes. Measured resonant frequency and Q factor were respectively 3.6 kHz and 1100 in the case of the excitation mode, and 4.0 kHz and 1400 in the case of the detection mode.

The response characteristics to angular rate were measured using the circuit shown in Fig. 11. A +90 deg. phase shift circuit and an auto gain control circuit were used for resonator excitation. The resonator vibrates at its resonant frequency and stabilized amplitude. The angular rate signal can be obtained by demodulating the detection mode signal with the driving signal. Figure 12 shows the electric charge output from the PZT thin film versus angular rate. In this measurement, the signal level for driving the piezoelectric

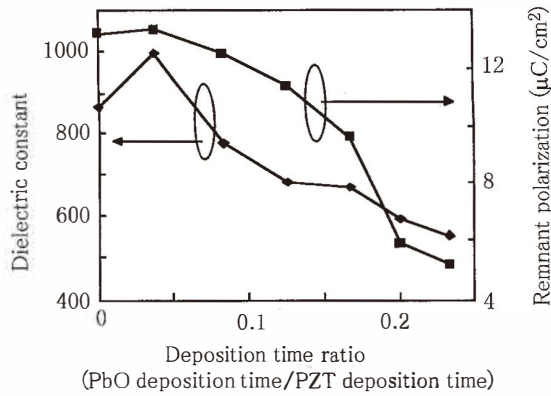


Fig. 8. Dielectric constant and remnant polarization versus deposition time ratio (PbO deposition time/PZT deposition time).

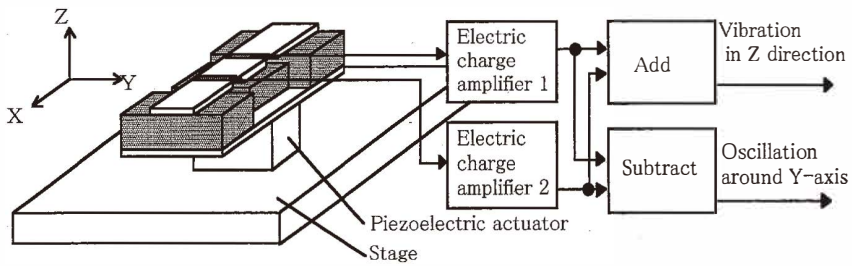


Fig. 9. Circuit block diagram for evaluation of piezoelectric properties and measurement of resonance characteristics of the sensor.

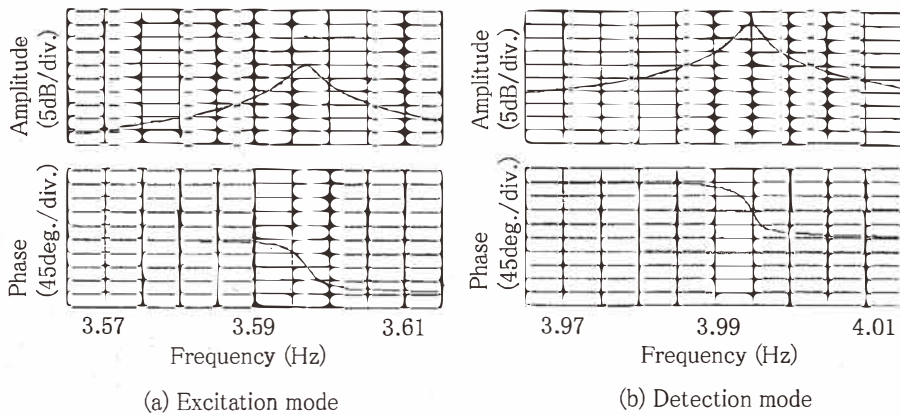


Fig. 10. Measured resonance characteristics of the sensor.

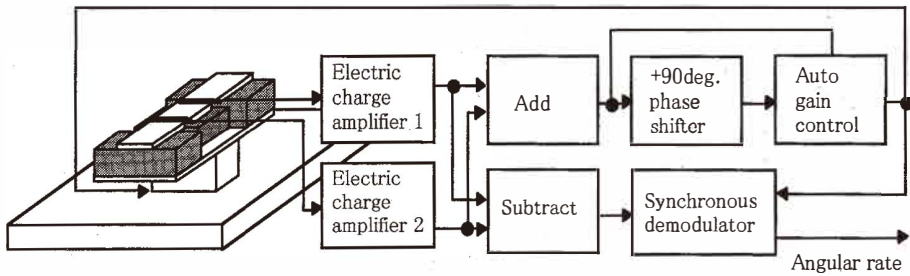


Fig. 11. Circuit block diagram for evaluation of angular rate detection.

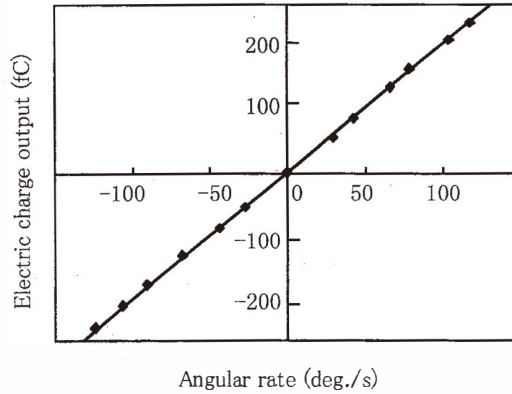


Fig. 12. Electric charge output from PZT thin film versus angular rate.

actuator was $1 V_{p-p}$. The vibration amplitude of the piezoelectric actuator was 65 nm_{p-p} . The sensitivity to angular rate was about $1.8 \text{ fC}/(\text{deg}/\text{s})$. The theoretical value that was calculated using the piezoelectric constant described above is $2.2 \text{ fC}/(\text{deg}/\text{s})$ and is close to the experimental value.

5. Conclusion

A silicon resonant angular rate sensor that uses PZT thin films for vibration detection was fabricated and examined. Since fabricated PZT films have poor piezoelectric characteristics ($1.44 \times 10^{-12} \text{ C}/\text{N}$), the film cannot be used for exciting sensor vibration. The sensor was driven by an external piezoelectric actuator instead of the PZT thin film. The sensor showed an angular rate sensitivity of about $1.8 \text{ fC}/(\text{deg}/\text{s})$.

Acknowledgment

This work was partly supported by a Grant-in-Aid (No. 07555125) from the Ministry of Education, Science, Sports and Culture, Japan.

References

- 1 M. Toyama, R. Kubo, E. Takata, K. Tanaka and K. Ohwada: *Sensors and Actuators A* **45** (1994) 125.
- 2 M. Sakata, S. Wakabayashi, H. Goto, H. Totani, M. Takeuchi and T. Yoda: *Proc. of IEEE Micro Electro Mechanical Systems Workshop* (San Diego, California, USA, Feb. 1996) p. 263.
- 3 M. Yamashita, K. Minami and M. Esashi: *Technical Digest of 14th Sensor Symposium* (Tokyo, Japan, 1996) p. 39.
- 4 M. Hashimoto, C. Cabuz, K. Minami and M. Esashi: *J. Micromech. Microeng.* **5** (1995) 219.
- 5 K. Maenaka and T. Shiozawa: *Transducers '93* (Yokohama, Japan, 1993) p. 642.